Developmental Science 3:1 (2000), pp 57–66

PAPER

The course of human events: predicting the timing of primate neural development

Barbara Clancy, Richard B. Darlington and Barbara L. Finlay

Cornell University, USA

Abstract

A recent model of the timing in which neural developmental events occur in a variety of mammals has shown high predictability of the order and duration of these events across species when appropriately computed. The model, originally derived to study the developmental mechanisms of evolutionary change in the nervous system, is adapted in this paper to predict the course of those events in the developing human, a sequence that has been difficult to determine using non-invasive neuroanatomical techniques. Using a modified version of our original regression model, we generate predicted times of occurrence for a large number of developmental events in the human embryo and fetus, and include a chart of comparable events for macaque monkeys. We discuss a bidirectional variability in the original model which allowed us to identify limbic and cortical primate neural events that are significantly deviant from the general mammalian norm, but which also proved predictable following modification. We test the modified model against empirically derived values for neural events not included in the original model, as well as through comparisons with human developmental sequences inferred by other methods. In view of the remarkable stability in the course of development across species, knowledge of the timing of human neural events need not be entirely restricted to the limited existent embryonic and infant data. Although the primate neural development sequence is somewhat more complex than that for other mammals, primate data continue to support a theory of developmental conservation across evolution.

Is it possible to apply the vast comparative neurodevelopmental literature to accurately predict development of the human brain? In contrast to the extensive data on neurogenesis and axonal growth in the developing brain of mammals such as rodent, carnivore and monkey, only scarce data are available on neurological events in the developing human since access to human nervous tissue is profoundly limited. Given that the single most practical goal of non-human research is a better understanding of the human brain, it is essential to determine pragmatic methods to relate the two. The sequence of developmental neurological events deserves close attention for a better understanding of effects of human genetic disorders or developmental disturbances. Ultimately, knowledge of the human neurodevelopmental sequence may allow optimal timing of diagnostic studies and/or intervention strategies.

Previous studies have linked neurodevelopmental timetables in non-humans to human developmental stages by extrapolating specific features of a well-studied species (e.g. neurogenesis in the rat) to those of humans using associations based on close examination of morphology (Bayer, Altman, Russo & Zhang, 1993) or through extrapolation from and interpolation between easily observed 'anchor events' such as eye opening (Robinson & Dreher, 1990) or weaning (Ashwell, Waite & Marotte, 1996). However, extrapolation of data from a single species through visual comparisons gleaned from a restricted number of human brains has obvious limitations, no matter how carefully done. Likewise, comparative studies using anchor events and interpolation can be confounded by variability in gestation time and dissimilar maturation at time of birth and weaning.

A different approach is to consolidate measurements of a large number of developmental events obtained from a variety of different mammalian species and use the associations to predict human events through appropriate modeling. In a series of recent studies, this

Address for correspondence: Barbara L. Finlay, Department of Psychology, Unis Hall, Cornell University, Ithaca, NY 14853, USA.

laboratory has drawn on data from the existing literature to successfully link the timing of neural events across several species (Finlay & Darlington, 1995; Finlay, Hersman & Darlington, 1998; Darlington, Dunlop & Finlay, 1999). Our data indicate that, despite wide ranges in gestation times and rates of maturation, the sequence of neurodevelopmental events remains remarkably stable across all studied species.

The most recent model (Darlington *et al*., 1999) uses observations of the timing of 92 different developmental events (such as neurogenesis and axonal outgrowth) obtained from nine placental mammalian species. Of the approximately 800 potential events in this matrix, about 40% have been empirically measured, although few have been identified in humans. The basic idea of this model is to derive a scale of developmental events (with later events scored high) and another scale of species (with slow-developing species scored high) such that the sum of any event score and any species score can be used to predict the timing of an event in that species. The model makes this sum fit a mathematical function of time, and the function we have derived is

$$\text{species score} + \text{event score} = \ln(\text{postconceptional day} - k).$$

The model was first described by Finlay and Darlington (1995), but by far the most complete published description of the procedures appears in Darlington *et al*. (1999). This regression model can be employed to estimate the date of any of the 92 developmental events in any of the nine species. Only 15 of these 92 events have been dated in the human brain, leaving a total of 77 unknown event dates. In the following study, the model was used to generate a time course for the entire set of events in the developing human. For comparative purposes, a similar sequence was generated for macaque, a closely related primate in which neural events are more easily observed such that 63 of the 92 events have been reported in the literature.

General mammalian model

The data set upon which the model is based includes neural event dates from nine eutherian mammals: mouse *Mus musculus*, hamster *Mesocricetus auratus*, rat *Rattus norvegicus*, spiny mouse *Acomys cahirinus*, rabbit *Oryctolagus cuniculus*, ferret *Mustela putorius furo*, cat *Felis domestica*, monkey *Macaca mulatta* and human *Homo sapiens*. Neural events include onsets, peaks and offsets of neurogenesis from a wide range of structures, peaks of neuronal death, development of major axon pathways, and aspects of process segregation and maturation. We found that some non-neural events such as birth and weaning do not fit the model, but others, such as eye-opening, fit well and are included.

Event dates were obtained from Tables 1–5 of Robinson and Dreher (1990), Table 2 from Finlay and Darlington (1995), Tables 1–3 of Ashwell *et al*. (1996), data reported in Dunlop, Tee, Lund and Beazley (1997) and Table 1 of Darlington *et al*. (1999).

In the model, species score + event score = ln(post-conceptional day $- k$), each species is given a score on a 'species scale' with hamster assigned the lowest score (0.565) and human the highest (2.5). Each developmental neural event is also assigned a score on an 'event scale'. For example, an early event such as the generation of neurons of brain stem motor nuclei is assigned a relatively low score of 0.789 while the peak of genesis for later born neurons of the superficial cortex scores higher at 1.857. (Score values are described in more detail below.) The constant (k) value takes into account that early neural organizational events (implantation, blastulation and differentiation of basic germinal layers) occur consistently in all species during the first days following conception. This constant has been somewhat modified as our database increased to a current value of 5.37 (Finlay & Darlington, 1995; Darlington *et al*., 1999). The additive constant was used in calculations of Y by applying the formula described in Finlay and Darlington (1995) and in more detail in Darlington *et al*. (1999):

$$Y = \ln(\text{day} - 5.37).$$

Employing a general linear model approach, we used eight dummy variables to distinguish between the nine species, and 91 dummy variables to distinguish the 92 events. To avoid a regression 'singularity' we omitted one species and one event from each list. This is standard practice as noted in any discussion of the general linear model (e.g. Darlington, 1990, ch. 10). We predicted Y (defined above) from these $91 + 8$ or 99 dummy variables. The regression slope computed for each dummy variable becomes the scale value for the corresponding species or event, with the 'base' species and event (the ones with no dummy variables) receiving scale values of 0. This procedure will typically produce some negative scale values, and will also produce some additive constant in the regression. (This additive constant is not the k value of 5.37 used in defining Y; it is completely different.) The model can then be simplified (made easier to use) in two ways without changing any of its predictions at all. One can eliminate the additive constant by adding its value to the species or event scale values, or a mixture of the two. This has the secondary benefit of making all the scale values

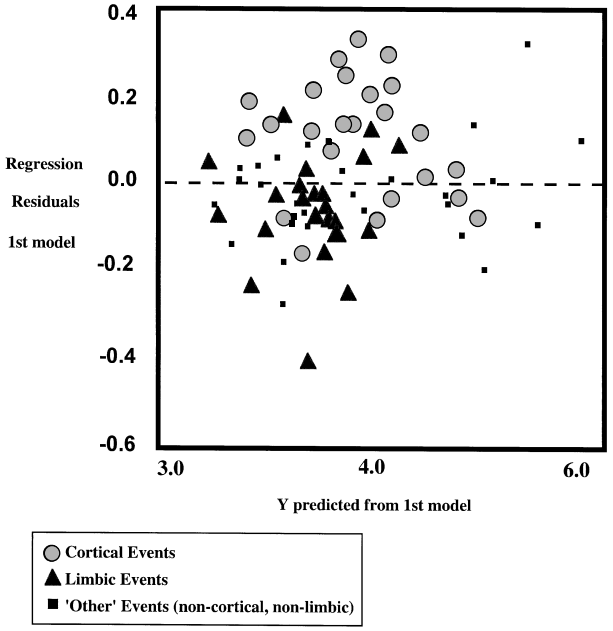

Figure 1 *Primate variability – original model. Primate regression residuals plotted against log-adjusted predicted days (Y) depicts variability in neural events in cortical (circles) and limbic (triangles) areas when using dates predicted by the unadjusted original model. The initial model predicted cortical events to occur somewhat earlier in primates than published observations indicated, while limbic events were predicted to occur rather earlier than observed.*

positive. We found an additive constant of 2.148, but eliminated it by adding 0.995 to every value on the event scale and adding 1.153 to every value on the species scale. These two values sum to 2.148, thus allowing us to ignore the additive constant. We chose these precise values because they produce a nice round number (2.5 exactly) for the human value on the species scale. We experimented to find the mathematical function of date which could best be predicted by this procedure. Of the functions we tried, the one that was most predictable in our sample of data was $Y = \ln(\text{postconceptional day} - 5.37)$; this function correlated 0.989 with the estimates of Y computed from the model.

For this study, the model was adapted to generate a human timetable for all 92 developmental events in the data set as follows:

$$\text{predicted postconceptional day} = \exp(\text{species scale} + \text{event scale}) + 5.37.$$

Substituting to predict, for example, the peak day of neurogenesis of ganglion cells in the human retina (species score 2.5; event score 1.415), the equation becomes: event day $= \exp(2.5 + 1.415) + 5.37$, establishing the predicted peak generation day at postconceptual (PC) day 55 of the 270–280 day human gestation. The

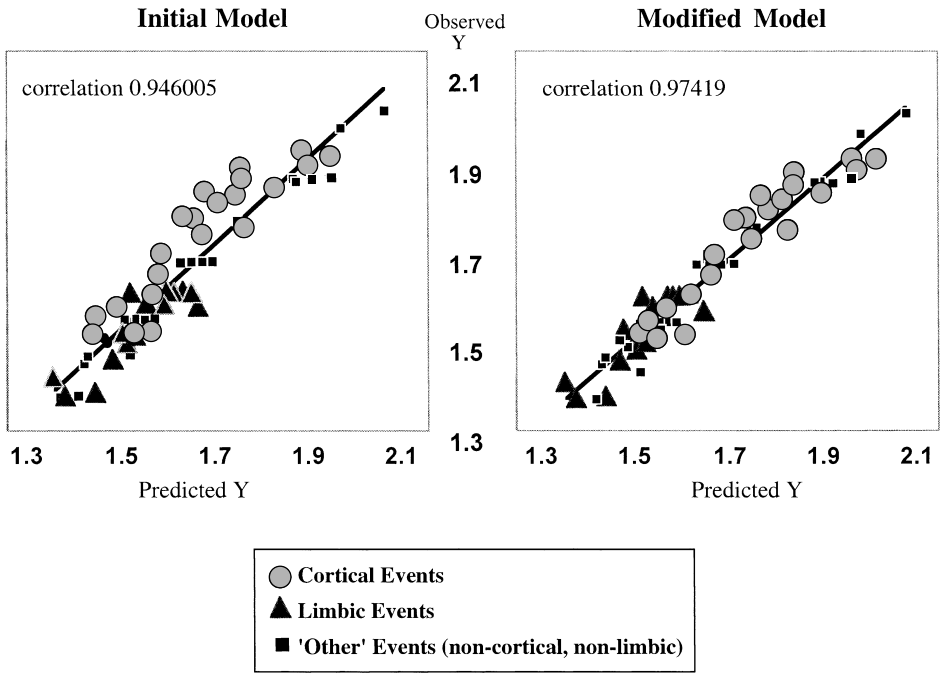

Figure 2 *Macaque neural events. Graphs depict tripartitioned predictions plotted against observations before and after adjustments were made to the model to account for limbic and cortical variability. Note that circles (representing cortical events) and triangles (representing limbic events) are both closer to the line in the modified version, indicating a decrease in variability. This decrease is also reflected in the higher correlation of the modified model.*

same formula can be used to determine event dates in any of the other species in the original study. Leaving the event scale unchanged at 1.415 while substituting macaque score (species score 2.285) into the above equation places the peak generation day of retinal ganglion cells at PC 43 of the shorter (165–170 day) macaque gestation. We discuss below how the original model was adjusted to account for two types of variability in the initial primate sequence generated by the model, a limbic factor and a cortical factor.

A modified primate model

To test the initial primate predictions, we compared log-transformed dates generated by the original model with log-adjusted raw data reported in the human and macaque developmental literature. The correlation between the 15 human observed and predicted dates was 0.9539. More relevant, since it was based on a higher number of observations (63 events), was the macaque correlation which was also acceptable at 0.943. These reasonably high correlations were somewhat expected since our previous work had convinced us of the predictability of neural event timing across species. However, a bidirectional distribution of certain variability in the primate data was intriguing. When dates predicted by the model could be compared with observed dates reported in the literature, we noticed that events reported to occur *earlier* than the model predicted were most often from neural areas associated with the limbic system, a group of distributed neural structures that includes the entire hippocampal formation, as well as regions associated with olfaction and emotion. Events observed *later* than predicted dates were generally isocortical events. The model-generated

Table 1 *Predicted human and macaque limbic event dates*

		Post-conceptional day			
Neural event	Event score	Macaque model	Macaque observed	Human model	Human observed
Locus coeruleus – peak	0.919	29	32[c]	36	
Magnocellular basal forebrain – peak	0.962	30	30[c]	37	
Reticular nuclei – peak	1.096	34		42	
Raphe complex – peak	1.105	34	30[c]	42	
Preoptic nucleus – peak	1.118	35		43	
Globus pallidus – peak	1.131	35		43	
Mammillo-thalamic tract appears	1.134	35		43	44[a]
Medial forebrain bundle appears	1.180	36	36[a]	45	33[a]
Suprachisamatic nucleus – peak	1.207	37		46	
Fasciculus retroflexus appears	1.218	38	40[a]	47	
Nucleus of lateral olfactory tract – peak	1.249	39		48	
Amygdala – peak	1.265	39	38[c]	49	
Stria medullaris thalami appears	1.297	40	48[a]	50	44[a]
Substantia nigra – peak	1.305	41	39[c]	50	
Anterior olfactory nucleus – peak	1.312	41		51	
Septal nuclei – peak	1.341	42	45[c]	52	
AV, AM and AD nuclei – peak	1.370	43		53	
Caudoputamen – peak	1.417	45	45[c]	56	
Subiculum – peak	1.429	45	48[c]	56	
Parasubiculum – peak	1.445	46	48[c]	57	
Fornix appears	1.463	47	48[a]	58	63[a]
Stria terminalis appears	1.471	47		58	56[a]
Presubiculum – peak	1.475	47	48[c]	59	
Dentate gyrus – peak	1.505	48	48[c]	60	
Anterior commisure appears	1.509	48	48[a]	60	70[a]
Entorhinal cortex – peak	1.529	49	48[c]	62	
CA 1, CA 2 – peak	1.530	49	48[c]	62	
Nucleus accumbens – peak	1.588	52	45[c]	65	
Tufted cells – peak	1.589	52		65	
Hippocampal commisure appears	1.616	53		67	77[a]
Isles of Calleja – peak	1.659	55		69	

Notes: In all tables, neural divisions for fiber tracts are based on the location of cells of origin. *Peak* refers to the peak day of neurogenesis, *start* and *end* to neurogenesis onset and offset.
Abbreviations: AD, anterodorsal; AM, anteromedial; AV, anteroventral; LGN, lateral geniculate nucleus; LGNd, dorsal lateral geniculate nucleus; SC, superior colliculus.
References: [a] Ashwell, Waite & Marotte, 1996; [b] Dunlop *et al.*, 1997; [c] Finlay & Darlington, 1995; [d] Robinson & Dreher, 1990.

data were examined using a regression model to plot variability. The resulting bi-modal pattern is illustrated in Figure 1 where a scatter plot of the regression residuals of 78 human and macaque events, plotted against log-adjusted data generated by the initial model, depicts consistent early limbic (triangles) and late cortical (circles) deviations. In the plot depicted in Figure 1, and in the graphs included in Figure 2, we have used log-transformed dates, effective in visually separating closely spaced information for clearer graphic presentation.

The positive and negative regularities in variability are not surprising since the entire data set upon which the model is based includes observations for three times as many cortical and limbic events in non-primates as in primates (69 : 18 cortical events; 68 : 23 limbic events). Thus there was a resulting bias in our initial model in favor of a non-primate mammalian developmental sequence. This deviation in developmental timing in primates maps directly onto a deviation in the relative size of the primate limbic system and isocortex compared with other mammals – the limbic system overall is smaller than would be expected for brain size in primates and the isocortex is larger (Finlay & Darlington, 1995; Kaskan & Finlay, 1999). We suggest here that the cause of the smaller limbic system in primates is this premature and relatively abbreviated neurogenesis, and the larger isocortex is due to its relatively delayed and prolonged neurogenesis.

Standard t residual analysis was used to measure the significance of the variability, focusing on events in developing primate cortical and limbic systems. Primate cortical events proved significantly positive ($t = 4.715$; $p = 0.000002$) indicating that these events reliably occur later in primates than the initial model predicted, while limbic events were significantly negative ($t = -1.874$; $p = 0.031$) indicating that they reliably occur earlier in primates than the initial model predicted (df = 240, one-tailed tests). Subsequent adjustments based on regression slopes were made to the original formula such that a small 'limbic value' of 0.0835 was uniformly subtracted from each primate limbic scale and a 'cortical value' of 0.2028 was added to the scale of all primate cortical events. Figure 2 depicts the lower variability in the macaque data produced following this modification, which also resulted in a higher correlation when comparing predicted events with published observations (log-transformed data; $r = 0.9742$).

The course of primate neural development

The adjusted model was applied to produce a timetable sequencing 92 human and macaque neural events. In the

Table 2 *Predicted human and macaque cortical event dates*

Neural event	Event score	Post-conceptional day			
		Macaque model	Macaque observed	Human model	Human observed
Subplate – start	1.290	40	40[d]	50	
Subplate – peak	1.319	41	43[c]	51	
External capsule appears	1.357	42	40[a]	53	56[a]
Cortical layer VI – start	1.410	44	45[d]	55	
Internal capsule appears	1.493	48	40[a]	60	63[a]
Cortical layer VI – peak	1.621	54	53[c]	67	
Cortical layer V – start	1.622	54	59[d]	67	
Optic axons invade LGN and SC	1.736	59		75	60[b]
Cortical layer V – peak	1.763	61	70[c]	76	
Cortical layer IV – start	1.786	62	70[d]	78	
Cortical layer VI – end	1.817	64	65[d]	80	
Cortical layer IV – peak	1.862	67	80[c]	84	
Cortical layer V – end	1.907	70	75[d]	87	
Corpus callosum appears	1.943	72		90	88[a]
LGN axons in subplate	1.970	74	78[d]	93	
Cortical axons reach LGN	1.996	76	67[d]	95	
Cortical layer IV – end	2.019	77	85[c]	97	
Cortical layer II/III – peak	2.021	77	90[c]	97	
Cortical axons innervate LGNd	2.159	88	82[d]	111	
Adultlike cortical innervation of LGN	2.316	102	96[d]	129	
Lateral geniculate axons in cortical layer IV	2.332	104	91[d]	131	
Visual cortical axons in superficial layers of SC	2.429	114	96[d]	144	

Note: See notes to Table 1.

Table 3 *Predicted human and macaque 'other' neural event dates (non-cortical, non-limbic)*

Neural event	Event score	Post-conceptional day			
		Macaque model	Macaque observed	Human model	Human observed
Cranial motor nuclei – peak	0.782	26		32	
Retinal ganglion cell generation – start	0.957	30	30[d]	37	
Inferior olivary nucleus – peak	0.985	31		38	
Red nucleus – peak	1.059	33		40	
Vestibular nuclei – peak	1.059	33		40	
Superficial SC laminae – start	1.060	33	30[d]	41	
Cranial sensory nuclei – peak	1.083	34		41	
Posterior commisure appears	1.093	34	35[a]	42	33[a]
LGNd – start	1.100	34	36[d]	42	
Medial geniculate nucleus – peak	1.185	37		45	
Purkinje cells – peak	1.199	37	39[c]	46	
Deep cerebellar nuclei – peak	1.215	38	38[c]	46	
Axons in optic stalk	1.218	38		47	51[b]
Ventrolateral geniculate nucleus – peak	1.227	38		47	
LGN – peak	1.281	40	43[c]	49	
Cochlear nuclei – peak	1.297	40		50	
Optic axons at chiasm of optic tract	1.313	41	36[b]	51	
Mitral cells – peak	1.324	41		51	
Ventroposterolateral and ventrobasal nuclei – peak	1.333	42		52	
Start of rapid axon gereration in optic nerve	1.339	42		52	
Retinal horizontal cells – peak	1.358	42	40[a]	53	
Claustrum – peak	1.361	43		53	
SC – peak	1.367	43	41[c]	53	
Dorsal lateral geniculate nucleus – end	1.383	43	43[d]	54	
Retinal ganglion cells – peak	1.410	44	43[c]	55	
Inferior colliculus – peak	1.452	46	43[c]	57	
Pontine nuclei – peak	1.503	48		60	
Optic axons reach LGN and SC	1.504	48		60	
Superficial SC laminae – end	1.544	50	56[d]	62	
Cones – peak	1.616	53	56[c]	67	
Retinal amacrine cells – peak	1.664	56	56[c]	70	
Retinal ganglion cell generation – end	1.717	58	57[d]	73	
Optic nerve axon number – peak	1.847	66	69[d]	83	
Superficial SC – start of lamination	2.129	86	86[d]	108	
Rods – peak	2.142	87	85[c]	109	
Retinal bipolar cells – peak	2.217	93	85[c]	117	
Ipsi/contra segregation in LGN and SC	2.304	101	87[d]	127	175[b]
Rapid axon loss in optic nerve ends	2.348	105	110[d]	133	
Eye opening	2.567	130	123[a,b,c]	164	182[a,b]

Note: See notes to Table 1.

accompanying tables, the predicted neural events are reported in PC days. The tables are arranged by neural area with fiber tract assignments based on the location of the cells of origin. Table 1 lists predicted limbic neural events in human and macaque, Table 2 lists predicted cortical events, while Table 3 includes 'other' neural events (non-limbic, non-cortical). Raw data obtained from the published literature are included when available.

Most neurogenesis takes place in the first trimester of human gestation. Over one-half of the generated human neural events are predicted to occur in human embryos during the second month of gestation (55 of 92), and many of the remaining events (28) are predicted to occur during the third gestational month (i.e. the beginning of the fetal period). A representative early developmental pattern is depicted for human visual events in Figure 3 where generated PC dates are noted alongside morphological outlines of the developing human eye and brain.

Testing the modified primate model

We have previously shown that our model is able to predict both late and early developmental events

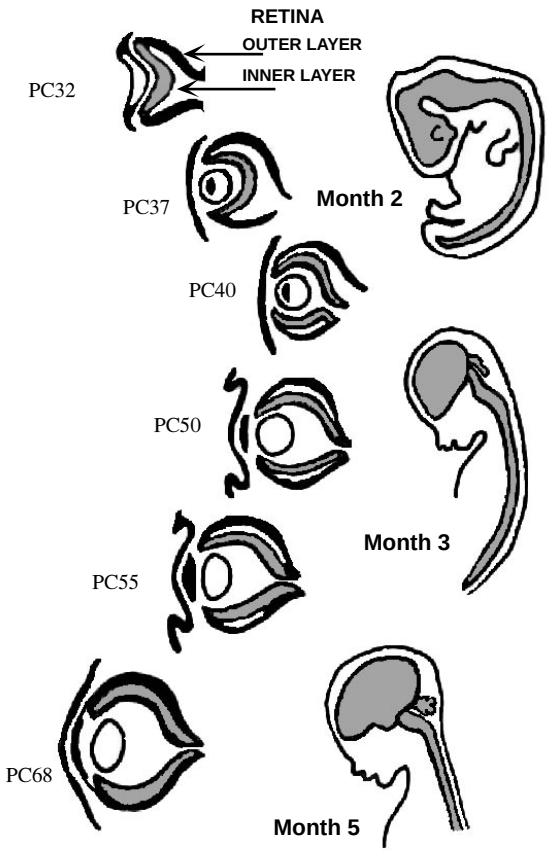

Month 2

retinal ganglion cell generation-start	PC 37
optic axons in optic stalk	PC 47
optic axons at chiasm of optic tract	PC 51
start of rapid axon gereration in optic nerve	PC 52
retinal horizontal cells-peak	PC 53
retinal ganglion cells-peak	PC 55
optic axons reach LGN and SC	PC 60

Month 3

retinal cones-peak	PC 67
retinal amacrine cells-peak	PC 70
retinal ganglion cell generation-end	PC 73
optic axons invade LGN and SC	PC 75
optic nerve axon number-peak	PC 83

Month 4

LGN axons in cortical subplate	PC 93
retinal rods-peak	PC 109
retinal bipolar cells-peak	PC 117

Month 5

LGN axons in cortical layer IV	PC 131
rapid axon loss in optic nerve ends	PC 133

Month 6

eye opening	PC 164

Figure 3 *Human visual events predicted from the model. The panel on the right lists representative visual events predicted using the model. The left panel depicts outlines of developing human eye and brain during embryonic and fetal ages. (Morphological outlines adapted from Lemire, Loeser, Leech & Alvord, 1975; and Martin & Jessell, 1991.)*

successfully (Darlington *et al*., 1999) and indeed, as shown above, predicted human and macaque sequences correlate favorably with existent primate data. However, correlations test only one aspect of variability; they cannot tell us in absolute terms how accurate the predictions produced by the model are likely to be. Errors in the original data set upon which the model is based are not only likely, they are inevitable. Observations will naturally suffer from differences among individual animals, rounding, and other sources of variation. There is also what we might call a 'delay' error due to the fact that a developing animal cannot be continuously observed. Consequently, the first date at which an event is observed is typically given as the event date for that species even though the event most probably occurred at some point prior to the observation. Human data may be particularly susceptible to delay error, since availability of human tissue is severely limited. Moreover, human embryonic ages can only be based on estimates of dates of fertilization so that physical measurements, rather than actual PC dates, are conventionally used in existent human studies. Therefore we have tested the dates generated by our model several ways – statistically, using t residuals and leverage-corrected residuals, and comparatively, using raw data not included in the original model and predictive data inferred by other methods. Confidence bands on predictions of individual observations, which allow for the fact that errors in measurement of the initial data – for whatever reasons – might cause our predicted dates to be estimated imperfectly, were also generated.

Confidence intervals

Classical statistical theories used to generate the predicted data control for sampling error, but some error remains based on a varying contribution of individual variation, observational error and specification error (failure to use a model with correct mathematical form), although it is not possible to know the relative importance of each. Using standard methods (Darlington, 1990, p. 355) we derived 95% confidence intervals for the average date each event occurs in humans. These intervals are depicted in the graph in Figure 4.

Analysis of errors

A *t* residual analysis was computed to test the model's distribution of error. All observations fell within statistically acceptable limits. Under an assumption of normally distributed errors, this indicates that any errors in the generated data fit a normal distribution pattern and as such are not considered significant.

Individual variation, observational error (especially likely for human observations) and specification error can all contribute to the differences between the observed data and our model's predictions of those same event dates. A fourth type of error caused by the lack of large samples for each primate event, sampling error, actually tends to lower these differences, due to the tendency of any statistical model to tailor itself to the precise data available and therefore to fit those data better than it would fit a new sample of data. Leverage-corrected residuals (LCRs) were computed to correct this problem (Darlington, 1990, p. 357; Darlington *et al.*, 1999). The root mean square error of the LCRs, which essentially provides an unbiased estimate of the residuals from a hypothetical true model derived from an infinitely large database, was 0.1309, in agreement with our model's estimated standard deviation of individual *Y* scores for each event (0.1326).

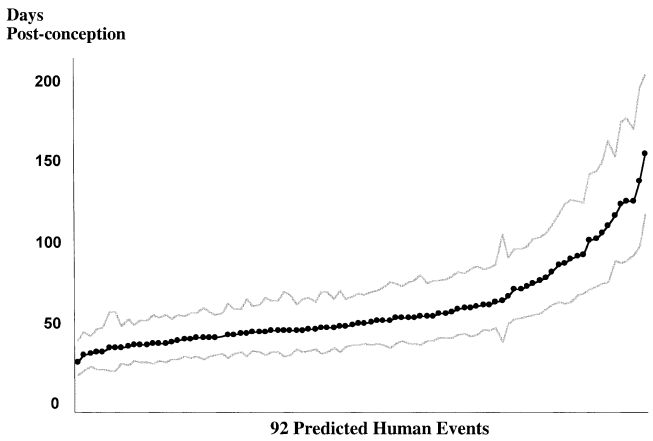

Figure 4 *Confidence intervals. Gray lines delineate estimated confidence limits for the predicted date on which each of the 92 events occur in humans (black circles).*

Comparisons of modified model predictions to morphologically generated predictions

Of the 77 unobserved human events produced by our model, 48 were the same events predicted in a detailed morphological study done by Bayer and colleagues (Bayer *et al.*, 1993). We compared our mathematically generated predictions with the predictions produced through Bayer's morphological comparison of rat and human brain. Some data in both series are in remarkable agreement; notably these are developmental events associated with non-cortical, non-limbic areas. However, a bidirectional variability was again demonstrated in the comparisons of these data sets. The disparity is illustrated in Figure 5 where comparative predictions for the 49 similar events have been tripartitioned into limbic, cortical, and 'other' (non-cortical, non-limbic) neural areas. Because our mathematical model produces a single date – either the start, stop, or peak date of the developmental event – predicted ranges of events from the morphological study were reduced to a single point prior to comparative analysis. One event (neurogenesis of hippocampal dentate neurons) was discarded due to an indeterminate termination date in the morphological study.

As shown in Figure 5, the morphological study consistently predicts cortical events to occur before the dates our adjusted model predicts – but in fact so early that many cortical events are predicted to occur in humans even earlier than they have been observed in the shorter macaque development (macaque 165–170 days gestation, human 270–280 days). Some limbic predictions in the morphological study show a similar, although inverted, incongruity with our mathematical predictions. These types of variability seem quite similar to the errors our initial (and also rodent-biased) model produced and underscore likely misinterpretations when extrapolating from a limbic, relatively non-cortical species to the highly corticalized primate.

Testing the model against new data

Another way to test the accuracy of the model is to compare the dates generated by our model with

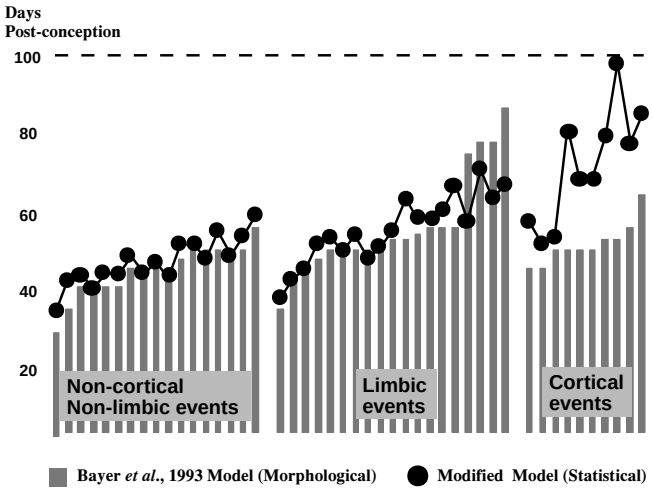

Figure 5 *Comparisons of predictions for human events. Our mathematical model, adjusted to account for variability in the timing of primate limbic and cortical development, is graphed with predictions from the morphological model of Bayer* et al. *(1993) in which rodent morphological data were compared to predict human neural events. The differences in cortical and limbic predictions between the two models may reflect a common difficulty encountered when extrapolating data from rodent to primate.*

observed data that were not reported in the original data set. The timing of cortical synaptogenesis, which we did not include in our original model, has been examined using correlated light and electron microscopic analysis (LM/EM) (Bourgeois & Rakic, 1993). Data from the LM/EM study indicate that the development of neural synapses in the human embryo begins in the cortical subplate and marginal zone at PC 50, the same day that our model indicates genesis of subplate neurons are at a peak. Synapses are reported to appear at PC 65 in layer VI of the cortical plate itself, again almost concurrent with the peak date of layer VI neurogenesis predicted by our model (PC 67). Similarly, our model predicts that the neurons of the human cortical plate have completed neurogenesis and extend axons into subcortical neural areas between PC 98 and 110, again consistent with Bourgeois and Rakic's (1993) report that at PC 112 human cortical neurons have assumed their mature laminar positions.

Studies on the genesis of cortical laminae in cingulate and motor areas during macaque development offer further support for the model-generated dates. Neurons of the motor cortex begin generation prior to the dates our model produces (Rakic, 1982) while cingulate cortex begins genesis before both motor cortex and model cortical predictions (Granger, Tekaia, Le Sourd, Rakic & Bourgeois, 1995). Taking into consideration that the cortical data in our model are based on events in posterior cortex, the model predictions match appropriately with the developmental gradient of mammalian cortex in which posterior cortex is generated following both anterior (motor) and more medial (cingulate) areas.

Subcortical neurogenesis predictions generated by our model are corroborated by combined autoradiographic and histological analysis of the midbrain of both monkey and human (Lenn, Halfon & Rakic, 1978). Lenn placed generation of monkey substantia nigra between PC 36 and PC 42, while human neurogenesis of the same area was found to occur between PC 43 and PC 55. Our model predicts the peak generation of neurons of the substantia nigra directly within these intervals – PC 41 for macaques and PC 50 for humans. Model-generated predictions are also in agreement with autoradiographic dopamine (DA) receptor studies which found the first DA receptors in human striatum to be expressed at PC 53 (Unis, Roberson, Robinette, Ha & Dorsa, 1997). Our model predicts neurogenesis in this area to peak 3 days later (PC 56).

Summary and conclusions

We have applied a comparative mammalian model to generate predictions for the course of neural developmental events in the human embryo and fetus. Regression formulas indicate that the predictions our model generates are statistically sound. Given the large amount of error in any one human observation, we might even suggest that our model may predict the average time of any one human event more accurately than can be done from an observation of that event in just one human subject. The modifications made to the initial model to account for bidirectional variability of primate limbic and cortical areas produce a somewhat more complicated developmental model for primates than that for non-primates. We should emphasize, however, that the overwhelming amount of variation in our sample is accounted for by factors common to all mammals and not just primates.

The sequence of neural events we have predicted for the developing human brain ends at eye-opening. Ironically, the timing of prenatal human neural development has proved to be easier to predict than that of postnatal development when behavioral information is readily available. Although the relative sequence of neural events is conserved across maturing mammalian species, absolute temporal variability increases rapidly following birth or eye opening. This is perhaps best represented by a difference of over 2 orders of

magnitude in the onset of sexual maturity across different mammals (approximate 12 years difference between rodents and humans) as contrasted to a relatively small difference of only 150 days in the timing of eye opening in the same mammals.

Nevertheless, the remarkable preservation of developmental event timing across evolution permits application of our comparative mammalian model to predict the course of early human events. In this way, the difficulties which arise when attempting to study the developing human brain may be surmounted and the sequence of prenatal human neurodevelopmental events confidently described. This knowledge is critical to help identify, understand and intervene in human developmental disorders. One clear conclusion that can be drawn from the data presented here is that a remarkably large number of generative and regressive neural events in the developing human occur during the very initial stages of gestation, with mature connective patterns established early in the second trimester. Although direct application of these data will require combined efforts of several disciplines, including medical science, genetics, developmental psychology and developmental neurobiology, it is hoped that diagnostic investigations and intervention strategies that require knowledge of the timing of human prenatal neural events may ultimately be performed with a relatively high degree of temporal accuracy.

Acknowledgements

The authors would like to thank Marcy Kingsbury and Peter Kaskan for their helpful comments. This work was supported by R01 NS19245 (BLF) and T32 MN19389 (BC).

References

Ashwell, K.W.S., Waite, P.M.E., & Marotte, L. (1996). Ontogeny of the projection tracts and commisural fibers in the forebrain of the tammar wallaby (*Macropus eugenii*): timing in comparison with other mammals. *Brain, Behavior and Evolution*, **47**, 8–22.

Bayer, S.A., Altman, J., Russo, R.J., & Zhang, X. (1993). Timetables of neurogenesis in the human brain based on experimentally determined patterns in the rat. *NeuroToxicology*, **14**, 83–144.

Bourgeois, J.-P., & Rakic, P. (1993). Changes of synaptic density in the primary visual cortex of the macaque monkey from fetal to adult stage. *Journal of Neuroscience*, **13**, 2801–2820.

Darlington, R.B. (1990). *Regression and linear models*. New York: McGraw-Hill.

Darlington, R.B., Dunlop, S.A., & Finlay, B.L. (1999). Neural development in metatherian and eutherian mammals: variation and constraint. *Journal of Comparative Neurology*, **411**, 359–368.

Dunlop, S.A., Tee, I.B.G., Lund, R.D., & Beazley, L.D. (1997). Development of primary visual projections occurs entirely postnatally in the fat-tailed dunnart, a marsupial mouse, *Sminthopsis crassicaudata*. *Journal of Comparative Neurology*, **384**, 26–40.

Finlay, B.L., & Darlington, R.B. (1995). Linked regularities in the development and evolution of mammalian brains. *Science*, **268**, 1578–1584.

Finlay, B.L., Hersman, M.N., & Darlington, R.B. (1998). Patterns of vertebrate neurogenesis and the paths of vertebrate evolution. *Brain, Behavior and Evolution*, **52**, 232–242.

Granger, B., Tekaia, F., Le Sourd, A.M., Rakic, P., & Bourgeois, J.-P. (1995). Tempo of neurogenesis and synaptogenesis in the primate cingulate mesocortex: comparison with the neocortex. *Journal of Comparative Neurology*, **360**, 363–376.

Kaskan, P.M., & Finlay, B.L. (1999). Encephalization and its developmental structure: how many ways can a brain get big? In. T. Sanderson (Ed.), *Evolutionary anatomy of the primate cerebral cortex*. Cambridge: Cambridge University Press.

Lenn, N.J., Halfon, N., & Rakic, P. (1978). Development of the interpeduncular nucleus in the midbrain of the Rhesus monkey and human. *Anatomy and Embryology*, **152**, 273–289.

Lemire, R.J., Loeser, J.D., Leech, R.W., & Alvord, E.C. (Eds) (1975). *Normal and abnormal development of the human nervous system* (pp. 196–204). Hagerstown, MD: Harper and Row.

Martin, J.H., & Jessell, T.M. (1991). Development as a guide to the regional anatomy of the brain. In E.R. Kandall, J.H. Schwartz & T.M. Jessel (Eds), *Principles of neuroscience* (pp. 296–308). Amsterdam: Elsevier.

Rakic, P. (1982). Early developmental events: cell lineages, acquisition of neuronal positions, and areal and laminar development. *Neurosciences Research Progress Bulletin*, **20**, 439–450.

Robinson, R.S., & Dreher, B. (1990). The visual pathway of eutherian mammals and marsupials develop according to a common timetable. *Brain, Behavior and Evolution*, **36**, 177–195.

Unis, A.S., Roberson, M.D., Robinette, R., Ha, J., & Dorsa, D.M. (1997). Ontogeny of human brain dopamine receptors I. Differential expression of (3H)-SCH23390 and (3H)-YMO9151-2 specific binding. *Developmental Brain Research*, **106**, 109–117.

Received: 7 May 2000
Accepted: 24 June 1999